PHYSICAL REVIEW B VOLUME 21, NUMBER 10 15 MAY 1980

(2×1) reconstructed Si(001) surface: Self-consistent calculations of dimer models

J. Ihm and Marvin L. Cohen
Department of Physics, University of California, Berkeley, California 94720
and Materials and Molecular Research Division, Lawrence Berkeley Laboratory, Berkeley, California 94720

D. J. Chadi
Xerox Palo Alto Research Center, Palo Alto, California 94303
(Received 21 December 1979)

The electronic structure of the (2×1) reconstructed Si(001) surface is studied using the self-consistent pseudopotential method. The calculation is based on the asymmetric-dimer model recently proposed by Chadi using the tight-binding method. The present calculation confirms that the asymmetric-dimer model results in a semiconducting surface in agreement with experiment. The density of states is calculated, and it compares favorably with experiment. A study of the charge distributions and the energy dispersions of surface states allows us to determine the character of individual surface states. By doing comparative calculations of the total energy of the symmetric and asymmetric dimers, we conclude that the latter is more stable because of exchange-correlation energy contributions.

I. INTRODUCTION

The atomic and electronic structures of clean silicon(001) surfaces constitute problems of great current interest because of their technological importance in solid-state devices. As early as 1959, the low-energy-electron-diffraction (LEED) measurements of Schlier and Farnsworth[1] provided evidence for a (2×1) reconstruction of the Si(001) surface. Subsequently, (4×2) LEED patterns were also observed.[2,3] The (2×1) reconstruction appears to be the dominant one[4-6] on Si(001) surfaces and the (4×2) on Ge(001) surfaces.[4] Recent work suggests[7] that the (2×1) and (4×2) reconstructions are similar in character differing only in the ordering of asymmetric dimers at the surface.

To explain the experimental observations, many distinct surface structural models for the Si(001) surface have been proposed.[1,4-12] Some of these are shown in Fig. 1; open circles denote surface atoms, and dark circles represent second-layer atoms. The ideal surface is shown in Fig. 1(a). In this configuration, there are two broken bonds per surface atom making the surface highly unstable. Pairing of surface atoms as shown in Fig. 1(b) reduces the number of dangling bonds by a factor of 2 and leads to a (2×1) periodicity. For the pairing (or dimer) model,[1,7,8,11] the surface-layer displacements can be chosen such that all bond lengths have their bulk values. Two different vacancy models[9,10] leading to a (2×1) surface are shown in Figs. 1(c) and 1(d). The doubling of the unit cell occurs in directions normal to or parallel to the zigzag chains at the surface for the two models. The "conjugated-chain model"[4] for the (2×1) surface and a variation of it are shown in Figs. 1(e) and 1(f) respectively. The dimer, vacancy, and conjugated-chain models have all been suggested at various times for explaining the surface structure of Si(001), but none have been found to be completely satisfactory. The calculated surface electronic densities of states for the vacancy[13] and conjugated chain models[14] are in disagreement with experimental photoemission spectra.[15,16] The dimer model gives better agreement[13]; however, all three models give metallic surface bands in disagreement with recent angle-resolved photoemission measurements.[16] Surface hydrogenation (and dehydrogenation through heating) yields a (2×1)-to-(1×1) conversion (and vice versa) which also suggests[17] that the (2×1) reconstruction does not result from vacancies. The pairing model was, therefore, reexamined, and it was shown[11] that the atomic distortions are not restricted to the surface layer but extend appreciably into the bulk. LEED calculations[6,12] for the new dimer model were found to be in much better agreement with the experimental data than for other models. The extent of the agreement was, however, not considered broad enough to regard the problem as completely solved.[12] In addition, the problem of metallic surface bands remained unchanged.[7]

Recent studies based on energy-minimization calculations[7] have shown that symmetric dimers as shown in Fig. 1(b) are unstable with respect to a buckling distortion. The formation of asymmetric dimers leads to partially ionic bonds between the paired atoms and, according to tight-binding (TB) calculations, to semiconducting surface bands. The top and side views of the asymmetric-dimer model are shown in Fig. 2. The atomic displacements (in Å) of the first two sur-

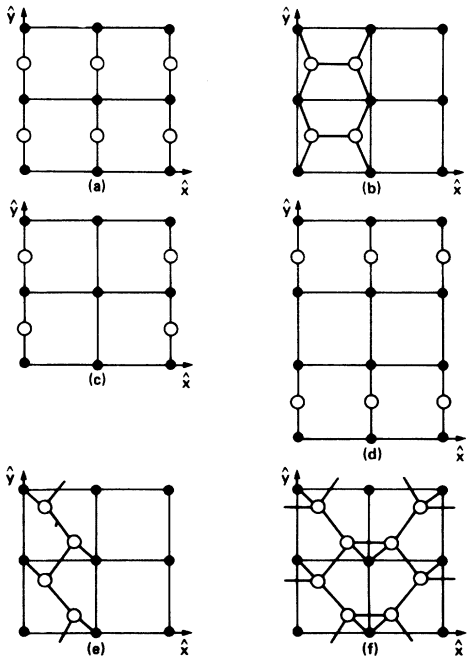

FIG. 1. Possible structural models for the Si(001) surface. Surface atoms are shown as open circles and second-layer atoms as solid circles. The structures shown correspond to (a) ideal unrelaxed surface, (b) pairing or (symmetric) dimer model, (c) and (d) vacancy models, and (e) and (f) conjugated-chain models.

face layers are[7] $\Delta X_1 = 0.46$, $\Delta X_2 = -1.08$, $\Delta Z_1 = 0.04$, and $\Delta Z_2 = -0.435$ as compared to $\Delta X_1 = -\Delta X_2 = 0.75$ and $\Delta Z_1 = \Delta Z_2 = -0.22$ for the symmetric dimer case. In the present paper, we take the asymmetric-dimer model for fully self-consistent pseudopotential calculations. Further relaxations up to the fifth layer from the surface are included in accordance with the TB calculations in Ref. 7, and comparisons are made between them.

The present calculation shows that the Si(001) surface in the asymmetric-dimer model is semiconducting. Other properties such as the density of states (DOS), the charge density, and the energy dispersion of surface states are studied in detail. The calculation of the total energy of this surface is attempted for the first time; the asymmetric dimer gives a lower energy than the symmetric case by 0.12 eV. In the next section, the calculational procedure is described. The results are presented in Sec. III, and summarizing remarks concerning the results are given in the last section.

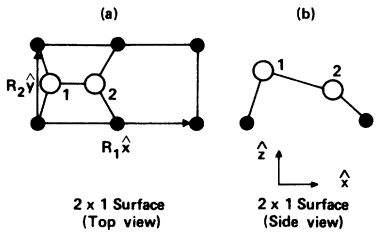

FIG. 2. Top and side views of an asymmetric-dimer geometry.

II. CALCULATIONS

The calculational procedure of the self-consistent pseudopotential method is outlined briefly below. Details of the method are to be found elsewhere.[18] The ionic pseudopotential representing the effective core-valence electron interaction is derived to reproduce the Si ionic and atomic spectra. The parametrized form of the pseudopotential in q space is

$$V(q) = (a_1/q^2)(\cos a_2 q + a_3)\exp(-a_4 q^4), \quad (1)$$

where $a_1 = -0.818\,786$ (the volume per Si atom is 189 a.u.), $a_2 = 0.790\,65$, $a_3 = -0.352\,01$, and $a_4 = -0.018\,07$. These values are given in rydberg atomic units. To facilitate the standard pseudopotential method, the repeated slab geometry simulating an actual surface is assumed. The unit supercell consists of ten layers of Si plus a vacuum region equivalent to five layers of Si in thickness. Si ions are reconstructed according to the model explained in the previous section. Once the structure of the Si ions is chosen, the valence electrons of Si are allowed to distribute themselves self-consistently. The $X\alpha$ method ($\alpha = 0.8$) is employed to calculate the exchange-correlation potential.

Because of the large unit cell (20 atoms plus a large vacuum region), we are limited by the matrix size in solving the Schrödinger equation. Plane waves up to 2 Ry in kinetic energy are included in the basis set (~200 plane waves), and another set of plane waves up to 5.5 Ry (~600 plane waves) are included through a second-order perturbation scheme. Self-consistent iterations with eight sampling points in the irreducible Brillouin zone are carried out until eigenvalues are stable up to 0.01 eV. At the final stage, the self-consistency is retested with 23 sampling points in the irreducible zone, and the same degree of stability is obtained. The latter sampling points are used to calculate the total charge density and the local density of states (LDOS). The LDOS curves are then smoothed to facilitate comparison with experiment. Two independent calculations are done, one with the asymmetric-dimer model and the other with the symmetric-dimer model. In the next section, we will concentrate on the results obtained from the asymmetric-dimer model. Comparisons will be made with the symmetric-dimer model and with the TB calculations.[7]

III. RESULTS

A. Electronic structure

The electronic structures for the asymmetric and symmetric dimer configurations are illustrated in Figs. 3–12. Figure 3 shows the self-consistent valence charge density of the asymmetric-dimer model. The charge density is plotted in the (110) plane perpendicular to the surface. At one layer below the surface, the charge density is essentially that of bulk Si. At the surface layer, on the other hand, the properties of the asymmetric dimer are dominant. Although the charge distribution of the new bond on the surface is not symmetric, the covalent nature of the bond is clearly evident in the figure. The maximum charge density of the bond (22.5 electons per bulk unit cell volume) is almost the same as that of the average bulk covalent bond (23). This is not surprising since the variation in bond lengths is maintained to within 2% in the present geometry in spite of the large rearrangement of the surface atoms. A small variation of the charge density (22.4 to 23.5) of the subsurface bonds suggests that there may be a slightly different geometry which could lower the energy.

Figure 4 illustrates the calculated projected band structure of Si projected onto the [001] direction. The surface-state bands of the asymmetric-dimer model are superimposed on the figure. Surface-state bands of the symmetric dimer are shown in the main gap region for comparison. Also inserted in the figure is the two-dimensional irreducible Brillouin zone of the (001) surface. The most striking feature in this plot is that the asymmetric-dimer model results in a semiconducting surface in contrast to the symmetric-dimer model. This confirms Chadi's[7] results using the empirical TB method. There are some differences in detail.

The self-consistent pseudopotential calculation gives ~0.1 eV for the indirect band gap while a larger value, (~0.6 eV) is obtained in the TB calculation; however, the direct gaps at Γ are the same (1 eV) in both calculations. The top of the

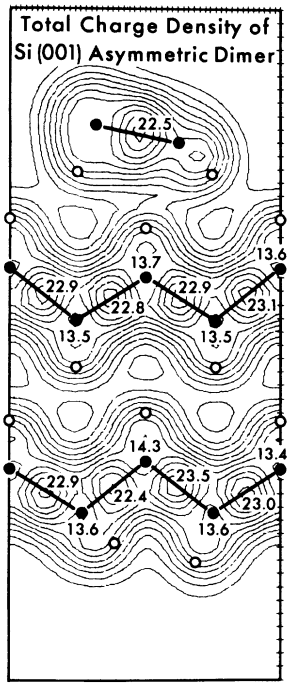

FIG. 3. Contour plot of the total valence-charge density for the asymmetric-dimer model plotted in a (110) plane cutting the surface at right angles. The solid circles represent the Si atoms lying on the plane, and the solid lines represent the hypothetical covalent bonds. Si atoms not on the plane are denoted by open circles. Normalization is determined by the number of electrons per bulk Si unit cell ($\Omega = 270$ a.u.), and the contour spacing is 2.

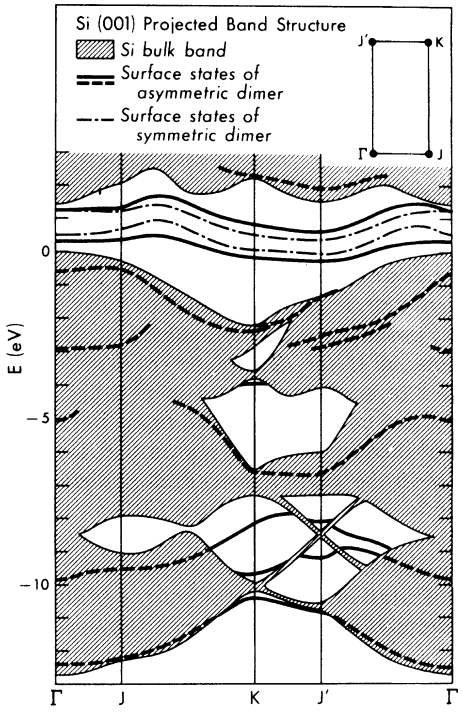

FIG. 4. The calculated band structure of bulk Si projected along the [001] direction (projected band structure). Bands of surface states of the asymmetric-dimer model are represented by solid lines; when these states merge with the bulk band continuum, they are denoted by broken solid lines. In the main gap region, the states for the symmetric-dimer model are shown (dash-dot lines) for comparison. The two-dimensional irreducible Brillouin zone for the (001) structure is given in the insert.

occupied surface-state bands occurs along JK in the Brillouin zone, but it is found at Γ in the TB calculation. For both the symmetric- and asymmetric-dimer models, the calculated (pseudopotential and TB) bandwidths are more than a factor of 2 wider than experiment (~0.3 eV).[16] In the formation of the asymmetric (ionic) dimer, the two overlapping surface state bands of the symmetric dimer are pushed away from each other until a small indirect gap opens up in the asymmetric model.

When forming the asymmetric dimer, the upper band shifts upward and the lower band shifts downward by an almost constant amount except for the region along ΓJ direction (Fig. 4). This is accompanied by a lowering of the Fermi level by ~0.2 eV. The top of the occupied bands occurs near J (slightly shifted toward K) at 0.5 eV above the valence-band maximum for Si bulk (E_v), and the bottom of the unoccupied bands occurs at J' with $E = 0.6$ eV above E_v. The asymmetric distribution of the charge is the driving force for the band shift. The lower occupied band corresponds to electronic states localized around the "up" atoms on the surface, and the upper empty band corresponds to states associated with the "down" atoms. This asymmetric distribution of the surface charge takes better advantage of the exchange-correlation energy than the more uniform charge distribution in the symmetric-dimer model without significantly increasing other contributions to the energy. This point will be discussed in more detail later.

In Fig. 5, the LDOS for the surface monolayer of the (a) asymmetric and (b) symmetric models and (c) the inner layer corresponding to Si bulk are presented.

Figures 5(a) and 5(b) are essentially the same in the valence band region. In the gap region, however, two peaks (E, F) corresponding to occupied and unoccupied surface states appear in (a) whereas one strong peak (E'), which is half filled, appears in (b). When comparing the calculated LDOS for the surface with photoemission results,[15] close agreement in the positions for the main peaks B and D is found. Not only are the locations of the peaks correct, but the shape of peak D is also in good agreement with experiment. The triangular shape of peak D is characteristic of the dimer models (symmetric and asymmetric).[15,16] The DOS of the vacancy model found in Ref. 13 or that of the conjugate-chain model in Ref. 14 shows a more or less squarelike peak in this energy region. There is disagreement between our calculations and experiment[15] for the positions of peaks A, C, and E. In our calculation, peak A is shifted toward higher energy in going from a bulk to a surface layer, but the photoemission data seem to agree with the bulk DOS (c) rather than the surface DOS (a). The relatively small peak C in Fig. 5(a) is not found in the photoemission experiment. This peak corresponds to weak surface resonances around $E = -5$ eV in Fig. 4. Again, the photoemission curve is in better agreement with the bulk DOS (c). It is possible that the matrix element for these states may be very small. Also, it is to be noted that we plot the LDOS for the surface *monolayer* while the photoemission experiment may probe a few layers inside the surface. As mentioned above, the agreement with experiment improves if we average the calculated LDOS of the surface layer (a) and inner layers (c). On the other hand, the position of the occupied dangling-bond states (E) is centered near E_v while the photoemission data show a shoulder at ~0.8 eV *below* E_v.[15] The question remains whether that shoulder corresponds to the dangling-bond states associated with up atoms.

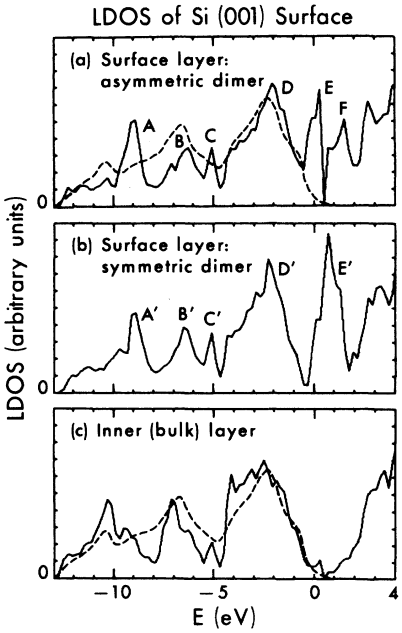

FIG. 5. The local density of states (LDOS) plots for the surface monolayer of the (a) asymmetric- and (b) symmetric-dimer models and for the (c) inner layer representing bulk Si. The experimental photoemission data of Ref. 15 are superimposed on the figure in dashed lines. The labeling of the peaks is explained in the text.

The calculation of the LDOS associated with a particular atom can be carried out more conveniently in a TB representation than in a plane-wave representation. An eigenfunction can be expressed in the TB method as a linear combination of the localized orbitals centered on each atom of

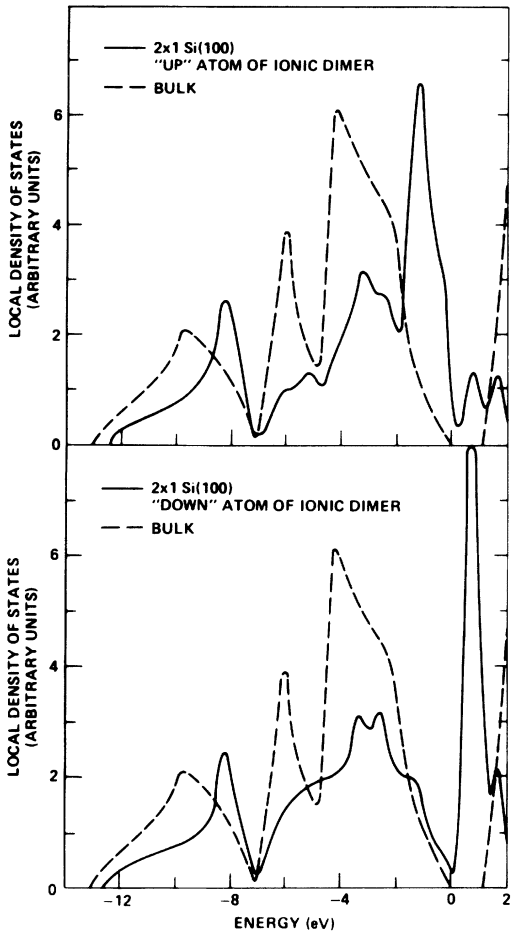

FIG. 6. The local density of states associated with the up and down atoms of the asymmetric dimer determined from TB calculations.

the system. Therefore, to study the electronic structure at the surface in more detail, the LDOS associated with up and down atoms of the asymmetric dimer obtained from the TB calculation[7] is shown in Fig. 6. The strong peaks near the valence-band maximum (top part of Fig. 6) and the conduction band minimum (bottom part of Fig. 6) correspond to the filled and empty dangling-bond surface states on the up and down atoms, respectively.

We now return to Fig. 4 and investigate individual surface states. A band of surface states (or resonances) exists at the bottom of the valence band throughout the Brillouin zone. These states split off from the bulk bands along KJ' whereas they merge into the bulk bands to become surface resonances in other regions of the Brillouin zone. Figure 7 shows a surface state at K. This is a back-bond state localized in the subsurface Si-Si bonding region. The corresponding state at J' is

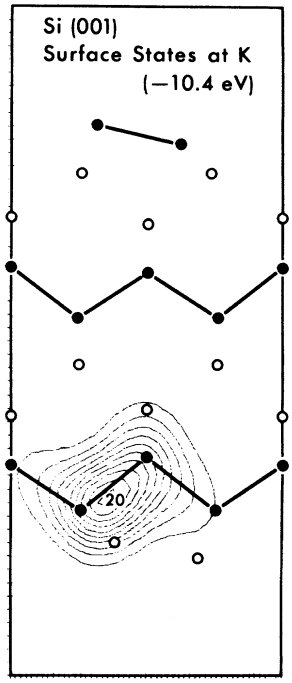

FIG. 7. Charge-density plot of the surface state at K (−10.4 eV) in the asymmetric-dimer model. The charge density is normalized to one electron per unit supercell. The plotting plane and notation are the same as in Fig. 3.

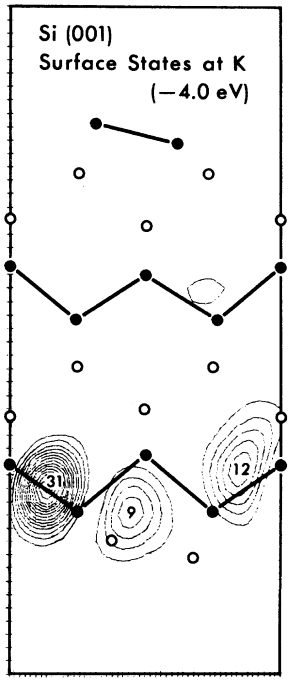

FIG. 8. Charge-density plot of the surface state at K (−4.0 eV) in the asymmetric-dimer model. The plotting plane, charge normalization, and notation are the same as in Fig. 7

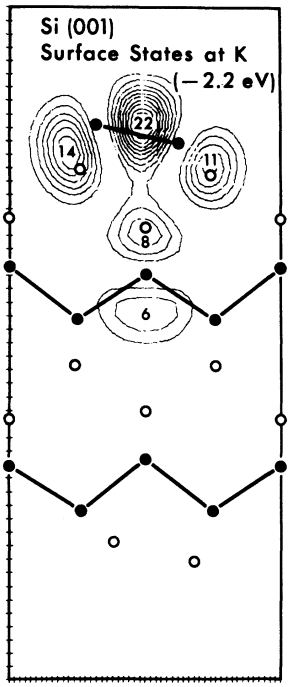

FIG. 9. Charge-density plot of the surface state at K (−2.2 eV) in the asymmetric-dimer model. The plotting plane, charge normalization, and notation are the same as in Fig. 7.

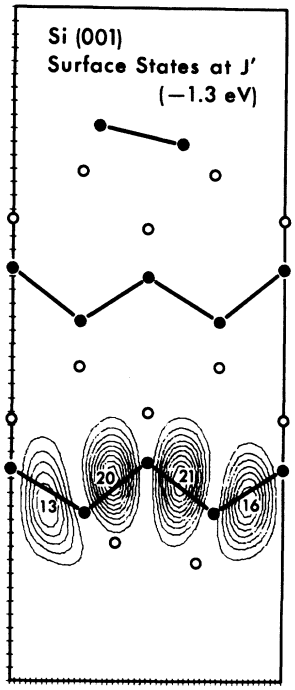

FIG. 10. Charge-density plot of the surface state at J' (−1.3 eV) in the asymmetric-dimer model. The plotting plane, charge normalization, and notation are the same as in Fig. 7.

similar in character.

There are two surface state bands in the −8 to −10 eV region. These two bands are connected at Γ where the states become resonances. They are mainly s-like states localized near the subsurface layer. A resonance band contributing a small peak at −5 eV in the LDOS curve of Fig. 5(a) exists in a wide region of the Brillouin zone. A strong p-like back-bond state appears in the "stomach" gap at K (−4 eV). Figure 8 illustrates the character of the state clearly. Localization of the charge is induced very strongly by the asymmetric reconstruction of the atoms. Otherwise, the charge would have been distributed evenly through the subsurface layer.

More surface resonances are found in the upper part of the bulk valence band. Two such states are shown here. A surface state at K (−2.2 eV) is presented in Fig. 9. This state is a covalent bond between P_z+P_x and P_z-P_x orbitals localized on the two atoms of the dimer (σ bonding). Figure 10 shows a back-bond p-like state at J' (−1.3 eV) which is not affected much by the asymmetric reconstruction and illustrates a rather even distribution of bonding charge in the subsurface layer.

The surface states in the gap are illustrated in Figs. 11 and 12. The lower band corresponds to

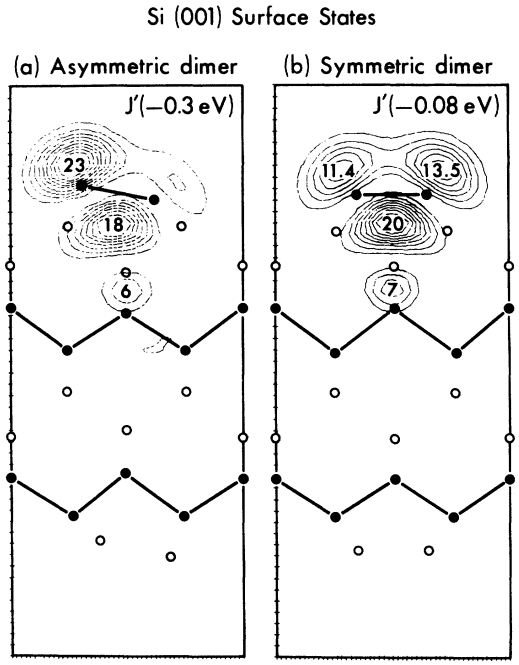

FIG. 11. Charge-density plots of the lower surface states band at J' in the (a) asymmetric- and (b) symmetric-dimer models. The plotting plane, charge normalization, and notation are the same as in Fig. 7.

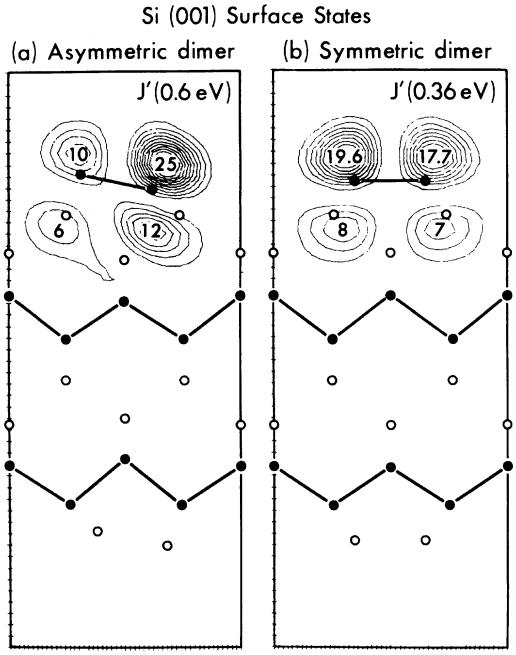

FIG. 12. Charge-density plots of the upper surface states band at J' in the (a) asymmetric- and (b) symmetric-dimer models. The plotting plane, charge normalization, and notation are the same as in Fig. 7.

the dangling-bond states of the up atom [Fig. 11(a)] as discussed before. This band is responsible for the large lobe of charge around the up atom in the total-charge-density plot (Fig. 3). Compared with a corresponding state of the symmetric dimer in Fig. 11(b), it becomes apparent how this state develops from a bonding state of P orbitals associated with each surface atom.

The upper unoccupied band corresponding to the dangling-bond states of the down atom is shown in Fig. 12(a). Again, compared with a corresponding state of the symmetric dimer in (b), it is easily recognized that this state originates from π antibonding of two P_z states associated with two surface atoms.

B. Total energy

We now turn our attention to the total energy of the system. The most fundamental way of determining the equilibrium configuration of the system is to minimize the total energy with respect to the structural degrees of freedom (at 0 K). The computational scheme for calculating the total energy in the self-consistent pseudopotential method has been formulated[19] and applied successfully to Si,[20] Mo, and W.[21] The empirical TB method was used[7] to show that the asymmetric dimer is lower in total energy than the symmetric dimer. However, self-consistency in charge distribution is required for a more accurate calculation because potential fluctuations are to be screened and reduced considerably through the self-consistency procedure.

In our plane-wave expansion scheme, the total energy per atom is[19]

$$E_{\rm tot}=\Omega_{\rm at}\Big(\sum_{i,\vec{G}}|\psi_i(\vec{k}_i+\vec{G})|^2(\vec{k}_i+\vec{G})^2+\tfrac{1}{2}\sum_{\vec{G}\neq 0}V_{\rm H}(\vec{G})\rho(\vec{G})+\tfrac{3}{4}\sum_{\vec{G}}\mu_{\rm xc}(\vec{G})\rho(\vec{G})+\sum_{\vec{G}\neq 0}S(\vec{G})U_{\rm ps}(\vec{G})\rho(\vec{G})\Big)+\alpha_1 Z+\gamma_{\rm Ewald}, \tag{2}$$

where $\Omega_{\rm at}$ is the atomic volume, Z is the valency, the $\vec{G}$'s are reciprocal lattice vectors, and $S(\vec{G})$ is the structure factor. $\psi_i(\vec{k}_i+\vec{G})$, $V_{\rm H}(\vec{G})$, $\rho(\vec{G})$, $\mu_{\rm xc}(\vec{G})$, and $U_{\rm ps}(\vec{G})$ are Fourier transforms of the electron wave function, the Hartree potential, the total (valence) charge density, the exchange-correlation potential, and the local pseudopotential. The index i represents both the wave vector $\vec{k}_i$, and band index n and runs over occupied states of the valence electrons. α_1 and $\gamma_{\rm Ewald}$ are

$$\alpha_1=\lim_{G\to 0}\Big(U_{\rm ps}(G)+\frac{8\pi Z}{\Omega_{\rm at}G^2}\Big)=\frac{1}{\Omega_{\rm at}}\int\Big(U_{\rm ps}(r)+\frac{2Z}{r}\Big)d^3r, \tag{3}$$

$$\gamma_{\rm Ewald}=\frac{1}{2}\Big(\sum_{\nu}{}'\frac{2Z^2}{|\vec{R}_\nu|}-\frac{1}{\Omega_{\rm at}}\int\frac{2Z^2}{r}d^3r\Big), \tag{4}$$

where the $\vec{R}_\nu$'s are lattice vectors to ionic sites. Hall's correction term[22] cancels with other electrostatic contributions and is not included in our definition of $\gamma_{\rm Ewald}$.[19] An alternative form for the total energy is

$$E_{\rm tot}=\sum_i\epsilon_i-\Omega_{\rm at}\Big(\tfrac{1}{2}\sum_{\vec{G}\neq 0}V_H(\vec{G})\rho(\vec{G})+\tfrac{1}{4}\sum_{\vec{G}}\mu_{\rm xc}(\vec{G})\rho(\vec{G})\Big)+\alpha_1 Z+\gamma_{\rm Ewald}, \tag{5}$$

where the ϵ_i's represent the eigenvalues of the valence electron wave functions. Equation (5) is used to calculate the total energy because this equation converges faster than Eq. (2) using second-order perturbation theory. $E_{\rm tot}$ here refers to the total crystal energy of the system; the crystal energy by definition excludes the energy in creating individual Si cores.

The result is summarized in Table I. Since our unit cell has 20 atoms and two "surfaces," the difference in total energy per atom between different geometries should be multiplied by ten to get the stabilization energy per dimer on the surface. A value of ~0.12 eV per dimer is obtained for the energy gain in going from a symmetric to an asymmetric model. This value is smaller than the one estimated in the TB calculation (~0.46 eV).[17]

TABLE I. The total energy of (2×1) reconstructed Si(001) surface simulated by the supercell geometry. The supercell geometry is explained in the text as well as in Ref. 7. The numbers correspond to the average total crystal energy per Si atom in rydberg. Therefore, to calculate the relative stabilization energy between two models per dimer, the difference of the total energy in the table (0.0009 Ry) should be multiplied by ten (the number of atoms in the unit cell divided by two because the unit cell has two surfaces).

Model	Asymmetric	Symmetric
Kinetic	2.384 42	2.380 07
$\Omega_{at}\sum' S(G)U_{ps}(G)\rho(G)$	−20.861 45	−21.061 76
$\alpha_1 Z$	1.023 69	1.023 69
$\frac{1}{2}\Omega_{at}\sum' V_H(G)\rho(G)$	9.809 79	9.915 07
$\frac{3}{4}\Omega_{at}\sum \mu_{xc}(G)\rho(G)$	−2.293 09	−2.291 89
γ_{Ewald}	2.074 81	2.173 87
Total	−7.861 83	−7.860 94

Considering that convergence of the present calculation is quite restricted because of the large unit cell, these values are not very accurately determined. It is also possible that other asymmetric reconstructions may yield even lower energies. Still, this calculation illustrates that the energy gain involved in the asymmetric reconstruction is of the order of 0.01 Ry. We note that the main contribution to the stabilization comes from the exchange energy. The exchange-correlation term contributes 0.012 Ry to the stabilization energy while all other terms contribute −0.003 Ry. It is convenient to think of the equilibrium configuration of the surface as the balance between the exchange-correlation energy and the classical contributions (kinetic and classical electrostatic energy). The exchange-correlation term tends to bring about bigger modulation in the charge distribution while the sum of the classical terms tends to suppress it.

IV. CONCLUSIONS

The present self-consistent calculation on a particular asymmetric-dimer model has been motivated by an earlier empirical TB calculation.[7] We have not studied all the possible reconstruction models here. Rather, the asymmetric-dimer geometry, which was found to give a semiconducting surface and a relatively low total energy in the TB calculations, is assumed for this more elaborate calculation of the electronic structure and the total energy. Various surface-state bands are found, and the character of these surface states is determined using charge-density plots.

With the present model, the surface is semiconducting, and the DOS is in better agreement with photoelectron data than any other models theoretically studied thus far. However, discrepancies between theory and experiment still exist, and all problems associated with the (2×1) reconstructed Si(001) surface are still not resolved.

ACKNOWLEDGMENT

The work at Berkeley was supported by the National Science Foundation (Grant No. DMR7822465) and by the Division of Materials Sciences, Office of Basic Energy Sciences, U. S. Department of Energy (Grant No. W-7405-ENG-48).

[1]R. E. Schlier and H. E. Farnsworth, J. Chem. Phys. 30, 917 (1959).
[2]J. J. Lander and J. Morrison, J. Chem. Phys. 37, 729 (1962).
[3]T. D. Poppendieck, T. C. Ngoc, and M. B. Webb, Surf. Sci. 43, 647 (1974).
[4]F. Jona *et al.*, J. Phys. C 10, L67 (1977).
[5]S. J. White and D. P. Woodruff, Surf. Sci. 64, 131 (1977).
[6]S. Y. Tong and A. L. Maldondo, Surf. Sci. 78, 459 (1978).
[7]D. J. Chadi, Phys. Rev. Lett. 43, 43 (1979); J. Vac. Sci. Technol. 16, 1290 (1979).
[8]J. D. Levine, Surf. Sci. 34, 90 (1973).
[9]J. C. Phillips. Surf. Sci. 40, 459 (1973).
[10]W. A. Harrison, Surf. Sci. 55, 1 (1976).
[11]J. A. Appelbaum and D. R. Hamann, Surf. Sci. 74, 21 (1978).
[12]F. Jona *et al.*, J. Phys. C 12, L455 (1979).
[13]J. A. Appelbaum, G. A. Baraff, and D. R. Hamann, Phys. Rev. Lett. 35, 729 (1975); Phys. Rev. B 14, 588 (1976).
[14]G. P. Kerker, S. G. Louie, and M. L. Cohen, Phys. Rev. B 17, 706 (1978).
[15]J. E. Rowe, Phys. Lett. 46A, 400 (1974); J. E. Rowe and H. Ibach, Phys. Rev. Lett. 32, 421 (1974).
[16]F. J. Himpsel and D. E. Eastman, J. Vac. Sci. Technol. 16, (1979) (in press).
[17]T. Sakurai and H. D. Hagstrum, Phys. Rev. B 14, 1593 (1976).
[18]M. Schlüter, J. R. Chelikowsky, S. G. Louie, and M. L. Cohen, Phys. Rev. B 12, 4200 (1975).
[19]J. Ihm, A. Zunger, and M. L. Cohen, J. Phys. C 12, 4409 (1979).
[20]J. Ihm and M. L. Cohen, Solid State Commun. 29, 711 (1979).
[21]A. Zunger and M. L. Cohen, Phys. Rev. B 19, 568 (1979).
[22]G. L. Hall, Phys. Rev. B 19, 3921 (1979).